Original Research *Neuroradiology/Head and Neck Imaging*

Volumetric analysis of maxillary sinus and assessment of various sinonasal anatomic variants on multi-detector computed tomography (MDCT) and their association with chronic rhinosinusitis

Aman Taneja[1] , Ankur Malhotra[1], Shruti Chandak[1] , Swasti Jain[1], Arpit Taneja[2] , Deepti Arora[3] , Swarna Laxmi[1] , Aishwarya Pandey[1]

[1]Department of Radiodiagnosis, Teerthankar Mahaveer Medical College and Research Center, Moradabad, Uttar Pradesh, [2]Department of Radiodiagnosis, Govind Ballabh Pant Hospital, New Delhi, [3]Department of Pathology, Teerthankar Mahaveer Medical College and Research Center, Moradabad, Uttar Pradesh, India.

*Corresponding author:
Ankur Malhotra,
Department of Radiodiagnosis,
Teerthankar Mahaveer Medical
College and Research Center,
Moradabad, Uttar Pradesh,
India.

drankur.m7@gmail.com

ABSTRACT

Objectives: The study aimed to evaluate the relationship between maxillary sinus volume and various sinonasal anatomical variants, as detected by multi-detector computed tomography, and their associations with chronic rhinosinusitis (CRS).

Material and Methods: A case–control study was conducted with 103 patients presenting with chronic sinonasal symptoms (cases) and 50 asymptomatic individuals (controls). A 128-slice computed tomography scanner was used to measure maxillary sinus volume and assess anatomical variants, such as a deviated nasal septum (DNS), concha bullosa (CB), and agger nasi cells. Exclusion criteria included previous sinonasal surgery, malignancy, craniofacial trauma, and lack of consent. Statistical analysis was performed using t-tests for continuous variables and Chi-square tests for categorical data. Receiver operating characteristic curve analysis was utilized to determine a DNS angle cutoff for predicting CRS.

Results: Anatomical variants were significantly more frequent in cases than in controls. The left-sided DNS was predominant in cases, while the right-sided DNS was more common in controls. The mean DNS deviation angle was notably larger in cases (10.84° ± 7.87) than in controls (5.55° ± 5.02). Maxillary sinus volume was significantly smaller in cases (9.69 cc on the left side and 10.23 cc on the right side) compared to controls (18.57 cc and 18.46 cc, respectively), with female patients exhibiting smaller volumes than males. Agger nasi cells were detected in 51.5% of cases versus 8.0% of controls. A strong association was found between CB and contralateral DNS. The optimal DNS deviation angle cutoff for predicting CRS was identified as 12.7°.

Conclusion: This study shows that CRS is linked to smaller maxillary sinus volumes, with males having larger sinus volumes than females. A DNS and larger deviation angles were associated with a higher risk of sinus inflammation, with angles over 12.7° predicting the onset of the condition. The presence of CB and agger nasi cells also contributed to the development of CRS.

Keywords: Maxillary sinus, Rhinosinusitis, Tomography

INTRODUCTION

Sinonasal illnesses, characterized by headaches and nasal symptoms, benefit from early detection and intervention.[1] Anatomical variations can obstruct airflow and contribute to recurrent sinusitis.[2] These variations may arise from genetic and environmental factors, and utilizing normative sizes aids in effective treatment planning.[3] Notably, variations such as agger nasi cells and concha bullosa (CB) complicate functional endoscopic sinus surgery (ESS),[4,5] highlighting the need for clear communication between radiologists and otorhinolaryngologists to mitigate surgical risks.[1]

While conventional radiography primarily serves as a screening tool, computed tomography (CT) scans provide critical anatomical insights that are essential for surgical planning, especially with advancements in multidetector CT.[3] CT imaging enhances visibility of variations such as Haller cells and CB, surpassing magnetic resonance imaging in detecting mucosal inflammation and fine bone structures.[6] Morphological changes evident on CT may predispose individuals to sinus-related diseases by narrowing ostio-meatal channels, thus obstructing mucus clearance and airflow.[7-9] Identifying these anatomical variations is crucial for surgical safety; common abnormalities include nasal septum deviation and CB.[10] A deviated septum can displace the middle turbinate, obstructing drainage and potentially causing issues on the contralateral side.[11] CB, an air-filled enlargement of the middle turbinate, is optimally detected by CT, revealing compression of the uncinate process and narrowing of the ethmoidal infundibulum, which can lead to maxillary sinus disease.[1]

The severity of rhinosinusitis is often linked to anatomical variations such as CB and a deviated septum.[10,12-14] A deviated septum frequently narrows the middle meatus, blocking drainage from the maxillary and frontal sinuses.[12] This restriction can hinder airflow, reduce oxygen pressure, and promote microbial growth, with changes in paranasal volume being associated with chronic sinusitis.[15,16] Furthermore, a deviated septum alters nasal aerodynamics, decreasing airflow on the convex side.[17] For assessing maxillary sinus capacity, 3D CT reconstruction is the most effective method for estimating volume.[18-20]

Studies outside India have compared maxillary sinus volume to age or the contralateral normal sinus in chronic rhinosinusitis (CRS) patients.[19,21] Some suggest a slight reduction in sinus capacity, while others find no significant correlation with size. Few studies have explored the link between sinus volume and anatomical variations, leading to controversial findings.[19,20,22,23] This study investigates sinonasal variations and estimates maxillary sinus volume using 3D CT, addressing gaps in research on the Indian population and the relationship between structural abnormalities and CRS.

MATERIAL AND METHODS

The study was conducted at Teerthanker Mahaveer Medical College and Research Center in Moradabad, within the Department of Radiodiagnosis, over a duration of 1.5 years. A case–control design was employed, recruiting 103 cases and 50 controls from the patient pool. Necessary approvals were obtained from the College Research Committee and the Institutional Ethical Committee to ensure compliance with ethical standards and research guidelines. During recruitment, potential participants were briefed on the study's objectives and procedures, and written informed consent was secured from all eligible individuals or their guardians.

Based on outcomes from a similar volumetric study of the maxillary sinus,[18] the sample size was calculated using the formula $n = ([Z\alpha/2 \times \text{S.D}]/E)^2$, where $Z\alpha/2$ was the standard normal variable (1.96 for a 95% confidence interval), Standard deviation (S.D) of outcome variable was 52, and E (Allowable error) was the allowable error of 10%. This calculation yielded a required sample size of 103 cases, with an additional 50 controls. Due to recruitment constraints during the 1.5-year study period, matching the number of controls to cases was not feasible. Nevertheless, the number of controls was deemed statistically adequate based on expert consultation and the methodology applied.

The study population included patients with symptoms suggestive of chronic sinonasal illness for the case group, while controls were patients referred for CT head scans without sinonasal symptoms. Exclusion criteria included previous sinonasal surgery, sinonasal malignancy, craniofacial trauma, and unwillingness to provide informed consent, ensuring the homogeneity and relevance of the study population.

Data collection techniques and tools

Technique of examination

The study utilized a 128-slice scanner (Ingenuity CT, Philips Healthcare, Best, The Netherlands) with patients positioned supine. A scanogram was obtained, and the imaging range extended from the highest level of the frontal sinuses to the base of the maxilla, covering an anteroposterior span from the posterior sphenoid bone to the anterior outer border of the frontal bone. Scan parameters included 120 kVp, 200 mAs, a slice thickness of 1 mm, a pitch of 0.391, and a reconstruction increment of 0.5 mm overlap. Following these configurations, CT scans of the paranasal sinuses (PNS) were performed. Advanced image reconstruction techniques were used to improve diagnostic quality, employing tools such as multiplanar reformation and volume calculation algorithms to analyze the images comprehensively.

Volume calculation

CT scan images from the full section series were utilized to estimate maxillary sinus volumes using Philips IntelliSpace 3D segmentation software [Figure 1a and b]. This software facilitated the creation of realistic images, provided a comprehensive anatomical understanding, and enabled precise volume calculations for each sinus.

Image interpretation

Images were evaluated using both bone and soft-tissue algorithms to identify various anatomical deviations, including deviated nasal septum (DNS), agger nasi cells, CB, Onodi cells, Haller cells, accessory maxillary ostia, and paradoxical middle turbinate, as well as pneumatized crista galli (wishbone). Careful examination was conducted in axial, coronal, and sagittal views to characterize these common sinonasal anatomical variants and assess mucosal thickening and opacification in the maxillary sinuses as potential indicators of sinus pathology.

Nasal septal deviation, observed on coronal CT scans, was quantified by measuring the angle formed between a line from the crista galli to the anterior nasal spine and a tangent to the most prominent point of the septal curvature [Figure 2]. This deviation was classified as mild (5°–10°), moderate (10°–15°), and severe (>15°).[24] A concha was identified by the presence of pneumatization in the middle turbinate and was categorized as unilateral or bilateral [Figure 3].[15] Onodi cells were air cells located posterior to the sphenoid sinus, extending superolaterally, while agger nasi cells were air cells located beneath the frontal sinus and anterior to the ethmoid sinus, often positioned inferomedial to the lacrimal bone.[25] Haller cells were defined as cells that grew into the bony orbital floor, forming the roof of the maxillary sinus [Figure 4a].[9] The paradoxical middle turbinate featured a convexity facing laterally [Figure 4b], and the pneumatized crista galli (wishbone) expanded from the adjacent frontal sinus [Figure 5].

Data collection and analysis were conducted by residents (A.T., S.J., A.P.) under the supervision of faculty members
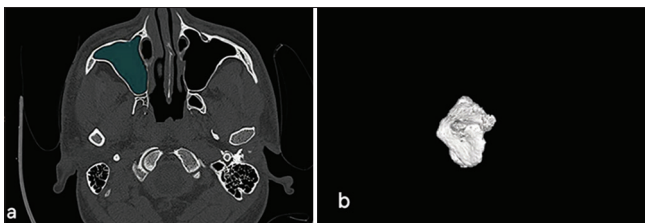

Figure 1: (a) Demonstrates the use of philips intelispace 3D segmentation software for calculating the volume of the left maxillary sinus, highlighting area of opacification. (b) Presents a 3D visualization of the sinus cavity.
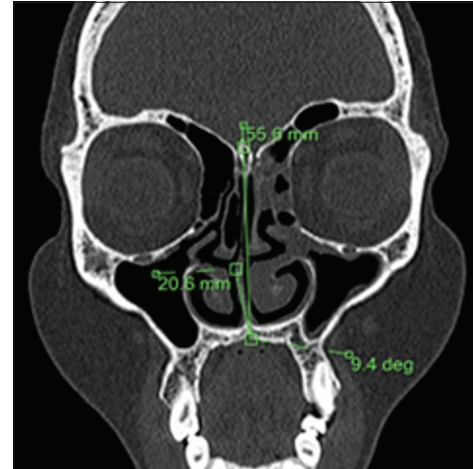

Figure 2: Coronal computed tomography scan illustrating the technique used to measure the degree of nasal septal deviation.
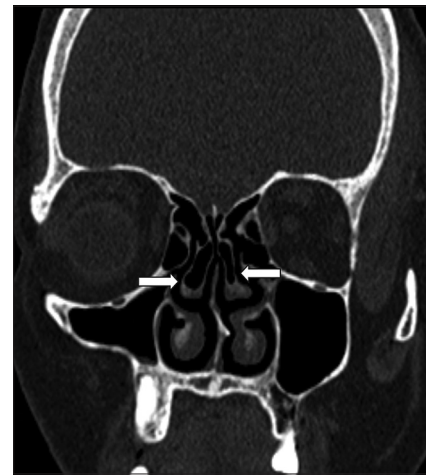

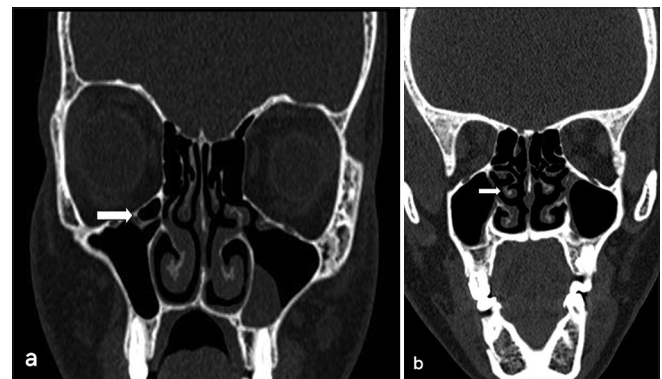**Figure 3:** Coronal computed tomography scan showing bilateral concha bullosa (white arrows).

Figure 4: (a) Coronal computed tomography (CT) scan displaying a right Haller cell with polypoidal mucosal thickening of the left maxillary sinus (white arrow indicates Haller cell). (b) Coronal CT scan displaying a right paradoxical middle turbinate (white arrow indicates the paradoxical middle turbinate).

Figure 5: Coronal computed tomography (CT) scan showing a pneumatized crista galli (wishbone) (white arrow indicates the pneumatized crista galli).

(A.M., S.C.), with a CT technician assisting in volumetric analysis using specialized software to ensure accuracy.

Statistical analysis

Data were analyzed using Microsoft Excel (Microsoft Corporation, NY, USA) and version 25.0 of the Statistical Program for the Social Sciences (SPSS). To ensure robust analysis, patients were profiled based on various demographic and etiological factors. For quantitative variables, normality was assessed, with parametric data analyzed using Student's t-test to compare means between groups, presented as mean ± standard deviation. For non-parametric data, the Wilcoxon–Mann–Whitney U-Test was utilized to compare independent samples. Qualitative variables were analyzed using the Chi-square test or Fisher's exact test, with results expressed as percentages. Box-and-whisker plots were employed to visualize data distribution and identify potential outliers. Receiver operating characteristic curves were generated to determine the optimal cutoff point for nasal septal deviation as a diagnostic criterion for CRS, with sensitivity, specificity, and diagnostic accuracy assessed from these curves. The significance level was set at $P < 0.05$ for all tests.

RESULTS

Out of 103 patients referred for CT scans of the PNSs and 50 controls without evidence of inflammatory sinus disease, data were collected, tabulated, and analyzed using SPSS version 25.0.

The age distribution of cases and controls indicates that the majority of both groups were young adults under 40 years, with cases ranging from 6 to 83 years and controls from 5 to 67 years. The mean age was 30.86 ± 15.36 years for controls and 30.55 ± 16.35 years for cases. Gender distribution revealed that among the 103 cases, 57 were male and 46 were female, resulting in a male-to-female ratio of 1.23:1, while females constituted 60% of the controls.

Symptomatology analysis showed that headache was the most commonly reported symptom (86%), followed closely by nasal discharge (84%), with facial pain reported in only 20.4% of cases.

Maxillary sinusitis was present in all cases, while frontal sinusitis was noted in 24.3%, ethmoid sinusitis in 14.6%, and sphenoid sinusitis in 2.9%, with some patients exhibiting them concurrently [Table 1].

Anatomical variations were prevalent, with DNS observed in 71% of cases compared to 62% of controls. Notably, agger nasi cells were present in 51.5% of cases but only in 8% of controls [Table 2].

Types of DNS varied, with the left-sided deviation being slightly more common among cases. Severity analysis indicated that most cases had a severe degree of nasal septal deviation (35%), whereas controls predominantly had mild deviations. The degree of nasal septum deviation was significantly higher in cases (10.84°) than in controls (5.55°), with $P < 0.001$ [Table 3]. The optimal cutoff value for the DNS angle predicting maxillary sinusitis was 12.7°, demonstrating a sensitivity of 53% and specificity of 94%, yielding an Area Under the Receiver Operating Characteristic of 0.713 [Figure 6].

Agger nasi cells were bilaterally present in 47.6% of cases but were mostly absent or unilateral in controls. CB was significantly more prevalent in cases (31.1%) compared to controls (14%) ($P < 0.05$). A significant correlation was observed between the presence of CB and contralateral DNS ($P = 0.02$).

The distribution of Onodi cells showed no significant difference between cases and controls ($P = 0.162$). In the cases, bilateral and right-sided Onodi cells were more frequently observed, while the left-sided occurrences were less common. In addition, no Onodi cells were identified in the control group.

The volumetric analysis indicated that the mean maxillary sinus volumes were significantly lower in cases compared to controls. The left-sided volumes averaged 9.69 cc in cases versus 18.57 cc in controls ($P < 0.001$) [Figure 7]. A similar volume difference was observed on the right side, where cases averaged 10.23 cc compared to 18.46 cc in controls ($P < 0.001$) [Figure 8]. In addition, male cases had a higher mean maxillary sinus volume than female cases, with a statistically significant difference noted on the left side. Overall, various anatomical variants, such as the presence of agger nasi cells and CB, were significantly more common in cases compared to controls, highlighting their potential role in the etiology of sinusitis.

Table 1: Distribution of sinuses involvement among cases.

Site of disease	Number of cases	Percentage
Maxillary Sinus	103	100
Frontal Sinus	25	24.3
Ethmoid Sinus	15	14.6
Sphenoid Sinus	3	2.9

Table 2: Prevalence of sinonasal anatomical variants in cases and controls.

Variation	Cases (%)	Controls (%)
Deviated nasal septum	71.0	62.0
Agger nasi cells	51.5	8.0
Concha bullosa	31.1	14.0
Onodi cells	10.7	0.0
Haller cells	4.8	0.0
Accessory maxillary ostia	4.8	0.0
Pneumatized crista galli (Wishbone)	2.9	0.0
Paradoxical middle turbinate	1.9	0.0

Table 3: Mean nasal septum deviation (degrees) in cases and controls.

Measurement	Cases	Controls	Wilcoxon-Mann-Whitney U-test
Mean (SD)	10.84 (7.87)	5.55 (5.02)	3674.500
Median (IQR)	12.9 (0–17.9)	6.6 (0–9)	
P–value			<0.001

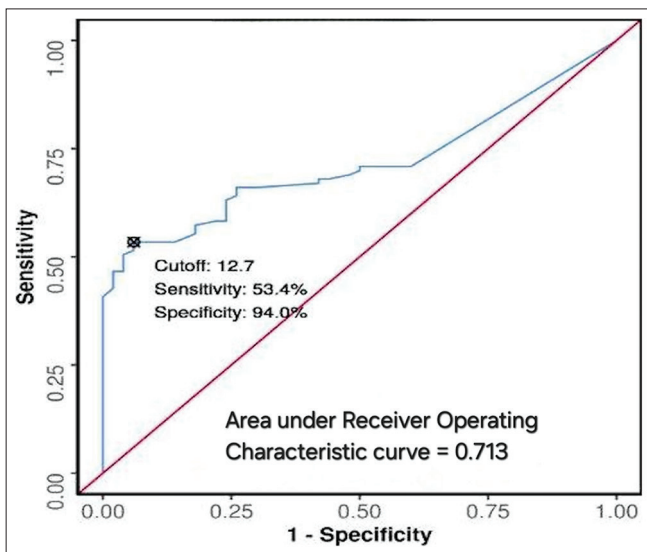IQR: Interquartile range, SD: Standard deviation

Figure 6: Receiver operative characteristics curve for nasal septal deviation angle as a predictor of maxillary sinusitis. ROC: Receiver operating curve.
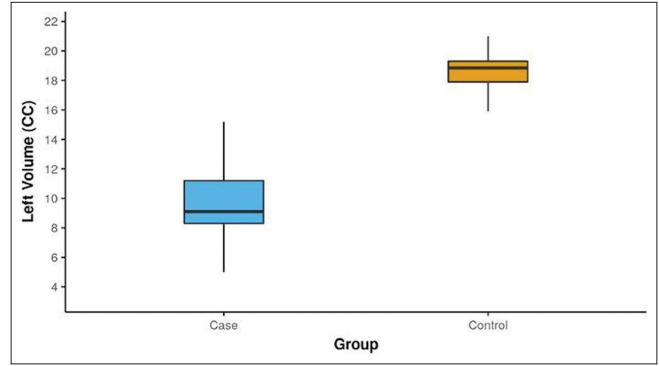

Figure 7: Box-and-whisker plot depicting the distribution of left maxillary sinus volume (CC) in cases and controls. The blue box represents the case group, while the yellow box represents the control group.
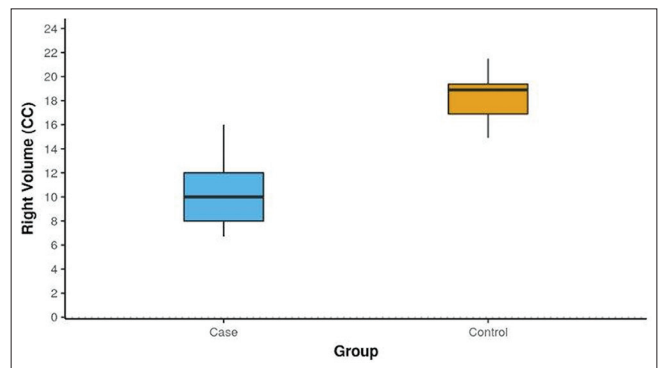

Figure 8: Box-and-whisker plot depicting the distribution of right maxillary sinus volume (CC) in cases and controls. The blue box represents the case group, while the yellow box represents the control group.

DISCUSSION

PNSs play a crucial role in reducing skull weight, humidifying air, and enhancing vocal resonance as nasal cavities expand, reshaping surrounding bones.[26] Given their complex anatomy and variability, understanding sinus architecture is vital for medical professionals, particularly in functional ESS.[27] This study demonstrates significant associations between various anatomical variants and maxillary sinusitis, notably the prevalence of DNS and reduced maxillary sinus volume. While conventional radiography offers limited insights, CT imaging provides detailed views, making it the preferred modality for assessing the PNSs. The integration of endoscopy and CT imaging has become the standard for evaluating PNSs, surpassing X-ray imaging.[28,29]

In CRS, reduced maxillary sinus volume indicates potential underlying pathophysiological changes exacerbated by chronic inflammation, impacting surrounding bone structure and worsening disease severity. This hypo-pneumatization complicates otolaryngology and dental surgeries, requiring

precise preoperative planning to optimize outcomes. Evaluating maxillary sinus volume through 3D CT scans provides critical information for surgical decision-making, aiding in managing developmental abnormalities and ensuring effective treatment strategies tailored to individual patient needs.

Age and sex distribution

Young individuals under 40 years comprised the majority of both cases and controls in this study. Controls ranged in age from 5 to 67 years, with a mean age of 30.86 ± 15.36 years, while cases ranged from 6 to 83 years, with a mean age of 30.55 ± 16.35 years. There was a slight male predominance among cases, consistent with earlier studies by Suresh *et al.*, Emirzeoglu *et al.*, and Thimmappa *et al.*[21,30,31] However, some investigations reported a modest female predominance, similar to the distribution among controls in this study. The male-to-female ratio among cases was 1.23:1, which aligns with previous findings.

Anatomical variations

Surgical treatment for sinonasal disorders has advanced significantly in recent decades. Traditional external procedures and prolonged hospital stays have been supplanted by minimally invasive techniques like ESS. ESS involves opening or enlarging obstructed sinus openings to restore normal airflow while preserving adjacent healthy mucosa and removing diseased tissue. The literature consistently reports favorable outcomes with ESS.[32,33] However, if surgical issues arise, they can pose significant risks and potential damage to nearby structures, such as the orbit and skull base, due to their close proximity.

In our analysis, the most prevalent anatomical variant in both cases and controls was DNS, consistent with earlier studies by Biswas *et al.*,[9] Pradeep *et al.*,[34] and Turna *et al.*[35] Agger nasi cells were the second most common, found in 51.5% of cases and 8.0% of controls, aligning with prior literature by Thimmappa *et al.*,[31] Lingaiah *et al.*,[27] and Pradeep *et al.*[34] CB was present in 31.1% of cases and 14.0% of controls, corroborating studies by Thimmappa *et al.* and Kucybała *et al.*[28,31]

In our study, the prevalence of Onodi cells in cases was found to be 10.7%, with none observed in the control group. This finding aligns with the previously reported prevalence range of 8-14%.[8,35] Left-sided Onodi cells were less common, while right-sided and bilateral occurrences were observed equally in cases. No significant difference was noted between cases and controls regarding the presence of Onodi cells, suggesting their limited clinical relevance in the development of chronic rhinosinusitis. However, our results contrasted with those of Ahanthem et al., who reported a higher prevalence of Onodi cells, attributing this discrepancy to their smaller sample size. [36]

Haller cells were found in 4.9% of cases, but none in controls, reflecting earlier studies by Gupta *et al.*,[37] Lingaiah *et al.*,[27]

and Biswas *et al.*[9] Accessory maxillary ostia were present in 4.9% of cases, lower than findings by Serindere *et al.*[6] The paradoxical middle turbinate, which exacerbates middle meatus constriction, was found in 1.9% of cases, consistent with Dakshina *et al.*[38] Pneumatized crista galli was present in 2.9% of cases, aligning with Turna *et al.*[35]

DNS and concha

Any deviation or change in the nasal septum's contour observed on coronal CT scans was labeled as DNS, categorized into mild (5°–10°), moderate (10°–15°), and severe (>15°).[24] Our research indicates a correlation between DNS and CB on the opposite side, consistent with findings by Kucybała *et al.*,[28] though Anazy[15] found no such link. The association between CB and DNS remains unclear, with theories suggesting a constant nasal air channel between the nasal septum and concha, causing the septum to deflect away from the concha due to factors beyond pressure.[8] Our findings suggest that the septum separates from the concha after its initial development, allowing the concha to enlarge to fill the expanded air channel.

Concha and inflammatory PNS disease

Conflicting data exist regarding the significance of concha in the development of sinusitis. While some authors argue that concha is not involved in sinusitis,[1,3,15] our investigation indicates a direct connection between concha presence and inflammatory sinus illness ($P < 0.05$), validating findings by Lakshmi *et al.*[39] This link may result from concha-induced compression on the uncinate process, leading to infundibular and middle meatal blockage or constriction.

DNS and inflammatory PNS disease

Vincent and Gendeh.[1] found that mild-to-moderate DNS alone does not predispose a person to inflammatory sinus illness. However, Javadrashid *et al.*[12] demonstrated that severe DNS is a significant risk factor for sinusitis. Our study also revealed a significant association ($P < 0.05$) between DNS and sinusitis, with higher degrees of DNS correlating with maxillary sinusitis. Severe maxillary sinusitis is linked to larger nasal septum deviations due to mechanical obstruction, impaired ciliary activity, and defective mucociliary transport, contributing to sinusitis pathophysiology.[40] In addition, a hypothesis suggests that craniofacial morphology in DNS patients might differ from those without variation, potentially representing a new risk factor for sinusitis.[41]

Cutoff point of DNS angle

The study calculated a threshold value for nasal septal deviation angle to distinguish between cases and controls

without maxillary inflammatory sinus disease, determining 12.7° as the optimal DNS angle cutoff value, with a sensitivity of 53% and specificity of 94% for maxillary sinusitis onset. Javadrashid *et al.*[12] established a lower cutoff value of 3.5° for discriminating inflammatory sinus disease presence, possibly due to ethnic differences and smaller sample size. Nonetheless, our findings align with Orlandi meta-analysis,[42] recommending a septal deviation angle of 10° to distinguish between positive and negative sinusitis cases.

Volumetric analysis

The PNS, being the largest cavity in the human skull, highlights the significance of its airspace. Thus, cavity volume remains the primary criterion for evaluating PNS anomalies, aiding in the objective definition of hypoplasia or sinus atelectasis. Various techniques have been employed to obtain volumetric data on the PNSs, such as quantifying volume using three-dimensional measurements or employing a square grid test procedure with different point densities.[21,43] While the previous studies utilized simple formulae for volume estimation, current research suggests a more meticulous approach, manually dividing each maxillary sinus slice-by-slice and reconstructing a 3D model to calculate bilateral volumes, as adopted in this study.[18,20] Although time-consuming, this method consistently yields accurate results, enhancing diagnostic precision.

Reports indicate that the maxillary sinus has the highest capacity, ranging from 8.6 to 24.9 cc.[44,45] In our study, the average maxillary sinus volume in cases closely resembled that found by Omer *et al.*, possibly due to similar age ranges of participants.[20] However, compared to our controls, the mean volume of the maxillary sinus in healthy patients was lower in studies by Emirzeoglu *et al.* and Sahlstrand-Johnson *et al.*, which may be attributed to racial features and the precision of volume assessment in our investigation.[30,46]

Gender differences in PNS diameters have been noted, with males typically having larger sinuses than females.[45,47] While some studies found no significant gender differences, others reported larger sinuses in males, consistent with our finding of larger maxillary sinus volumes in men, especially on the left side.[21,44] Recent research comparing volumes of diseased PNSs with unaffected controls yielded inconclusive results, but studies on CRS patients indicated smaller sinuses compared to the normal population, consistent with our findings of smaller maxillary sinus volumes in CRS patients.[16,20,44]

Limitations of this research include the modest sample size and single-center design, which may reduce the statistical significance of our findings. In addition, the homogeneous Northern Indian patient population limits the generalizability of our results to other ethnic groups. The complexity of calculating maxillary sinus volume using 3D CT techniques in high-volume settings presents challenges; radiologists require significant practice to achieve accuracy, potentially delaying clinical integration. However, once mastered, these techniques hold the promise of improving patient outcomes and effectively guiding clinical decisions.

While our study focused on anatomical variations and their association with CRS, it did not directly examine environmental factors such as dust, air pollution, and seasonal variations, which can affect the prevalence and severity of sinonasal diseases. Future studies should include these factors for a more comprehensive understanding of sinonasal health in the context of CRS.

CONCLUSION

Our study employed a precise method to calculate maxillary sinus volume, revealing reductions associated with CRS and highlighting gender disparities. The prevalence of a DNS was noted, with greater deviation angles correlating with inflammatory maxillary sinus conditions. Notably, a deviation angle exceeding 12.7° served as a predictive marker for disease onset. In addition, the presence of CB and agger nasi cells significantly influenced disease development. These findings underscore the critical importance of thorough anatomical evaluation in clinical practice, particularly in understanding and managing CRS and its associated anatomical variations.

Declaration of patient consent

The authors certify that they have obtained all appropriate patient consent.

Conflicts of interest

There are no conflicts of interest.

Use of artificial intelligence (AI)-assisted technology for manuscript preparation

The authors confirm that there was no use of artificial intelligence (AI)-assisted technology for assisting in the writing or editing of the manuscript and no images were manipulated using AI.

REFERENCES

1. Vincent TE, Gendeh BS. The association of concha bullosa and deviated nasal septum with chronic rhinosinusitis in functional endoscopic sinus surgery patients. Med J Malaysia 2010;65:108-11.
2. Fadda GL, Rosso S, Aversa S, Petrelli A, Ondolo C, Succo G. Multiparametric statistical correlations between paranasal sinus anatomic variations and chronic rhinosinusitis. Acta Otorhinolaryngol Ital 2012;32:244-51.
3. Smith KD, Edwards PC, Saini TS, Norton NS. The prevalence of concha bullosa and nasal septal deviation and their relationship to maxillary sinusitis by volumetric tomography. Int J Dent 2010;2010:404982.
4. Kennedy DW, Zinreich SJ. The functional endoscopic approach to inflammatory sinus disease: Current perspectives and technique modifications. Am J Rhinol Allergy 1988;2:89-96.
5. Stammberger H, Posawetz W. Functional endoscopic sinus surgery. Concept, indications and results of the Messerklinger technique. Eur Arch Otorhinolaryngol 1990;247:63-76.
6. Serindere G, Gunduz K, Avsever H. The relationship between an accessory maxillary ostium and variations in structures adjacent to the maxillary sinus without polyps. Int Arch Otorhinolaryngol 2022;26:e548-55.
7. Bolger WE, Butzin CA, Parsons DS. Paranasal sinus bony anatomic variations and mucosal abnormalities: CT analysis for endoscopic sinus surgery. Laryngoscope 1991;101:56-64.
8. Stallman JS, Lobo JN, Som PM. The incidence of concha bullosa and its relationship to nasal septal deviation and paranasal sinus disease. AJNR Am J Neuroradiol 2004;25:1613-8.
9. Biswas J, Patil CY, Deshmukh PT, Kharat R, Nahata V. Tomographic evaluation of structural variations of the nasal cavity in various nasal pathologies. Int J Otolaryngol Head Neck Surg 2013;2:129-34.
10. Mohebbi A, Ahmadi A, Etemadi M, Safdarian M, Ghourchian S. An epidemiological study factors associated with nasal septum deviation by computed tomography scan: A cross sectional study. BMC Ear Nose Throat Disord 2012;12:15-20.
11. Masood A, Moumoulidis I, Panesar J. Acute rhinosinusitis in adults: An update on current management. Postgrad Med J 2007;83:402-8.
12. Javadrashid R, Naderpour M, Asghari S, Fouladi DF, Ghojazadeh M. Concha bullosa, nasal septal deviation and paranasal sinusitis; a computed tomographic evaluation. B-ENT 2014;10:291-8.
13. Bora A, Koc M, Durmus K, Altuntas EE. Evaluating the frequency of anatomical variations of the Sinonasal region in pediatric and adult age groups according to gender: Computed tomography findings of 1532 cases. Egypt J Otolaryngol 2021;37:58.
14. Yazici D. Evaluation of anatomical variations on paranasal sinus CT. ENT Updates 2018;8:175-9.
15. Anazy FH. The incidence of concha bullosa and its association with chronic rhinosinusitis, deviated nasal septum and osteomeatal complex obstruction. Bahrain Med Bull 2011;33:4-9.
16. Ikeda A. Volumetric measurement of the maxillary sinus by coronal CT scan. Nihon Jibiinkoka Gakkai Kaiho 1996;99:1136-43.
17. Subramanian S, Lekhraj Rampal GR, Wong EF, Mastura S, Razi A. Concha bullosa in chronic sinusitis. Med J Malaysia 2005;60:535-9.
18. Pérez Sayáns M, Suárez Quintanilla JA, Chamorro Petronacci CM, Suárez Peñaranda JM, López Jornet P, Gómez García F, *et al.* Volumetric study of the maxillary sinus in patients with sinus pathology. PLoS One 2020;15:e0234915.
19. Aşantoğrol F, Coşgunarslan A. The effect of anatomical variations of the sinonasal region on maxillary sinus volume and dimensions: A three-dimensional study. Braz J Otorhinolaryngol 2022;88 (Suppl 1):S118-27.
20. Omer A, Yousef M, Ali Omer MA, Zidan MM, Abbas W. Volumetric analysis of the paranasal sinuses using CT among chronic sinusitis conditions. Int J Sci Res 2020;9:1550-4.
21. Suresh KS, Jehan M, Kumar A. Measurements of maxillary sinus volumes and dimensions by computed tomography scan for gender determination. J Anat Soc India 2014;63:36-42.
22. Al-Rawi NH, Uthman AT, Abdulhameed E, Al Nuaimi AS, Seraj Z. Concha bullosa, nasal septal deviation, and their impacts on maxillary sinus volume among Emirati people: A cone-beam computed tomography study. Imaging Sci Dent 2019;49:45-51.
23. Senturk M, Azgın I, Ocal R, Sakarya EU, Güler I, Övet G, *et al.* Volumetric analysis of the maxillary sinus in pediatric patients with nasal septal deviation. ENT Updates 2016;5:107-12.
24. Periyasamy V, Bhat S, Sree Ram MN. Classification of naso septal deviation angle and its clinical implications: A CT scan imaging study of Palakkad population, India. Indian J Otolaryngol Head Neck Surg 2019;71:2004-10.
25. Souza RP, Junior JP, Tornin OD, de Souza Tornin O, de Oliveira Paes Junior AJ, de Barros CV, *et al.* Sinonasal complex: Radiological anatomy. Radiol Bras 2006;39:367-72.
26. Miranda CM, Maranhão CP, Arraes FM, Padilha IG, Farias LP, Jatobá MS, *et al.* Anatomical variations of paranasal sinuses at multislice computed tomography: What to look for. Radiol Bras 2011;44:256-62.
27. Lingaiah RK, Puttaraj NC, Chikkaswamy HA, Nagarajaiah PK, Purushothama S, Prakash V, *et al.* Anatomical variations of paranasal sinuses on coronal CT-scan in subjects with complaints pertaining to PNS. Int J Anat Radiol Surg 2016;11:215-9.
28. Kucybała I, Janik KA, Ciuk S, Storman D, Urbanik A. Nasal septal deviation and concha bullosa - do they have an impact on maxillary sinus volumes and prevalence of maxillary sinusitis? Pol J Radiol 2017;82:126-33.
29. Bhattacharyya N, Fried MP. The accuracy of computed tomography in the diagnosis of chronic rhinosinusitis. Laryngoscope 2003;113:125-9.

30. Emirzeoglu M, Sahin B, Bilgic S, Celebi M, Uzun A. Volumetric evaluation of the paranasal sinuses in normal subjects using computer tomography images: A stereological study. Auris Nasus Larynx 2007;34:191-5.

31. Thimmappa TD, Amith P, Nagaraja M, Harsha KN, Gangadhar KS, Azeem A. Anatomical variations of sinonasal region: A CT scan study. Int J Res Med Sci 2014;2:1441-5.

32. Hindi K, Alazzawi S, Raman R, Prepageran N, Rahmat K. Pneumatization of mastoid air cells, temporal bone, ethmoid and sphenoid sinuses. Any correlation? Indian J Otolaryngol Head Neck Surg 2014;66:429-36.

33. Salhab M, Matai V, Salam MA. The impact of functional endoscopic sinus surgery on health status. Rhinology 2004;42:98-102.

34. Pradeep K, Rakesh BS, Prasad R. Anatomical variations of sinonasal region: A coronal CT scan study. Int J Contemp Med Res 2016;9:23-7.

35. Turna O, Ayabar MD, Karagoz Y, Tuzcu G. Anatomic variations of the paranasal sinus region: Evaluation with multidetector CT. Istanbul Med J 2014;15:104-9.

36. Ahanthem N, Basvaraju MS, Pachipulusu B, Pravin GU. Assessment of anatomical variations of paranasal sinus region: A computed tomography study. Int J Oral Care Res 2017;5:97-101.

37. Gupta S, Gurjar N, Mishra HK. Computed tomographic evaluation of anatomical variations of paranasal sinus region. Int J Res Med Sci 2016;4:2909-13.

38. Dakshina DM, Rao R, Rao SP. Analytical study of anatomical variations of nose and PNS in CT scan and chronic sinusitis. IOSR JDMS 2016;15:30-5.

39. Lakshmi YV, Singh TD, Fathima R, Kumar VH. Incidence of concha bullosa and its role in chronic rhinosinusitis. Int J Otorhinolaryngol Head Neck Surg 2021;7:1279-83.

40. Luo X, Liang C, Xu K, Tang S, Ren X, Liu D. Influence of nasal septal deviation on incidence of bilateral sinusitis. Lin Chuang Er Bi Yan Hou Tou Jing Wai Ke Za Zhi 2012;26:777-80.

41. Bachert C. Experimental studies of the effect of nasal respiratory obstruction on ventilation of the maxillary sinus. Laryngol Rhinol Otol (Stuttg) 1986;65:250-5.

42. Orlandi RR. A systematic analysis of septal deviation associated with rhinosinusitis. Laryngoscope 2010;120:1687-95.

43. Masri AA, Yusof A, Hassan R. A three-dimensional computed tomography (3D-CT): A study of maxillary sinus in Malays. CJBAS 2013;2:125-34.

44. Sánchez Fernández JM, Anta Escuredo JA, Sánchez Del Rey A, Santaolalla Montoya F. Morphometric study of the paranasal sinuses in normal and pathological conditions. Acta Otolaryngol 2000;120:273-8.

45. Thomas A, Raman R. A comparative study of the pneumatization of the mastoid air cells and the frontal and maxillary sinuses. AJNR Am J Neuroradiol 1989;10:S88.

46. Sahlstrand-Johnson P, Jannert M, Strömbeck A, Abul-Kasim K. Computed tomography measurements of different dimensions of maxillary and frontal sinuses. BMC Med Imaging 2011;11:8.

47. Nitinavakarn B, Thanaviratananich S, Sangsilp N. Anatomical variations of the lateral nasal wall and paranasal sinuses: A CT study for endoscopic sinus surgery (ESS) in Thai patients. J Med Assoc Thai 2005;88:763-8.